NASA CR-73699

Department of AERONAUTICS and ASTRONAUTICS
STANFORD UNIVERSITY

Theoretical Considerations of Some Nonlinear Aspects of Hypersonic Panel Flutter

by

S. C. McIntosh

Second Annual Report

NASA Grant NGR 05-020-102

1 September 1966 to 31 August 1967

Theoretical Considerations of Some Nonlinear Aspects of Hypersonic Panel Flutter

by

S. C. McIntosh

Second Annual Report

NASA Grant NGR 05-020-102

1 September 1966 to 31 August 1967

TABLE OF CONTENTS

NOTATION

a	Panel chord or beam length
$\bar{a}_k$	Modal amplitude for transverse displacement
a_k	Dimensionless modal amplitude, $\frac{\bar{a}_k}{h}$
A	Amplitude parameter
$\bar{b}_0, \bar{b}_R, \bar{b}_k$	Modal amplitudes for in-plane displacement
B	Amplitude parameter
D	Plate modulus, $\frac{Eh^3}{12(1-\nu^2)}$
D_Q	Beam shear modulus
E	Modulus of elasticity
$(F_x)_k$	Generalized force associated with k^{th} in-plane mode
$(F_z)_k$	Generalized force associated with k^{th} transverse mode
h	Panel thickness
I	Beam area moment of inertia about neutral axis
K	Running spring constant, panel in-plane restraint spring
M	Free-stream Mach number
N	Number of assumed modes for transverse displacement
p	Pressure
p_∞	Free-stream pressure
$\overline{\Delta p}$	Static pressure difference across panel; positive if cavity pressure exceeds free-stream pressure
Δp	Dimensionless static pressure difference, $\frac{\overline{\Delta p}\, a^4}{Dh}$
q	Free-stream dynamic pressure, $\frac{\rho U^2}{2}$
$\tilde{Q}$	Shear-force amplitude: $Q(x,t) = \tilde{Q}(x)e^{i\omega t}$
$\bar{R}_x$	Applied in-plane load
R_x	Dimensionless applied in-plane load, $\frac{\bar{R}_x a^2}{D}$
t	Time

T	Kinetic energy
$\bar{u}$	In-plane displacement
U	Free-stream speed
$\bar{w}$	Transverse displacement
$\tilde{w}$	Amplitude of transverse displacement: $\bar{w}(x,t) = \tilde{w}(x)e^{i\omega t}$
W	Potential energy
x	In-plane (axial) coordinate
z	Transverse coordinate
α	In-plane restraint parameter, $\frac{Ka}{[Eh+Ka(1-\nu^2)]}$
γ	Gas constant for free stream
λ	Dimensionless dynamic-pressure parameter, $\frac{2qa^3}{MD}$
μ	Dimensionless mass ratio, $\frac{\rho a}{\rho_m h}$
ν	Poisson's ratio
ρ	Free-stream mass density
ρ_m	Panel or beam mass density
τ	Dimensionless time, $t\left(\frac{D}{\rho_m h a^4}\right)^{\frac{1}{2}}$
ω	Frequency
$(\dot{-})$	Derivative of dimensional quantity with respect to t
$(')$	Derivative of dimensionless quantity with respect to τ

I. INTRODUCTION

This report presents a summary of the second year's research activity under NASA Grant NGR 05-020-102, monitored technically by the Nonsteady Phenomena Branch of Ames Research Center. The purpose of this research program is to study in a systematic manner the effects on panel response and stability of nonlinear (nonviscous) aerodynamic loading at hypersonic Mach numbers. It is of particular interest to determine whether or not nonlinear aerodynamic effects will provide a theoretical explanation for experimentally observed nonlinear behavior, as discussed below in Section III.

The equations of motion for a panel (plate-column) on hinged supports, with both aerodynamic and panel geometric nonlinearities, are derived and discussed in detail. Representative solutions for various cases are then presented, including an unanticipated diversion into the problem of interpreting results for zero system damping. Additional sections deal briefly with the work performed on a clamped panel and on methods of analysis, and a final section discusses topics of research to be considered during the next year.

II. PANEL ON HINGED SUPPORTS

2.1 Equations of Motion

Consider the two-dimensional panel, or plate-column, illustrated in Fig. 1. The supports are hinged, and the in-plane motion at one end is resisted by a distributed spring whose running spring constant is K. Free-stream parameters shown are the Mach number M and the dimensionless dynamic-pressure parameter λ. The panel is loaded by an applied in-plane load $\overline{R}_x$, a static pressure difference $\overline{\Delta p}$, and an unsteady pressure difference $p - p_\infty$. The unsteady pressure is approximated in hypersonic flow by the second-order piston-theory expression

$$p - p_\infty = \frac{2q}{M}\left[\frac{1}{U}\frac{\partial \overline{w}}{\partial t} + \frac{\partial \overline{w}}{\partial x} + \frac{(\gamma+1)M}{4}\left(\frac{1}{U}\frac{\partial \overline{w}}{\partial t} + \frac{\partial \overline{w}}{\partial x}\right)^2\right] \tag{2.1}$$

Here $\overline{w}(x,t)$ is the middle-surface transverse displacement of the panel, and q is the free-stream dynamic pressure. Since the pressure acts normal to the instantaneous panel surface, there arise in a rigorous sense both transverse and in-plane aerodynamic loads when the panel deflection is finite. Order-of-magnitude consistency then dictates including both a transverse aerodynamic load $p - p_\infty + \overline{\Delta p}$ and an in-plane aerodynamic load $[(p - p_\infty)_L + \Delta p]\frac{\partial \overline{w}}{\partial x}$, where the subscript L denotes the linear part of the unsteady pressure expression in Eq. (2.1).

The panel transverse displacement is represented as a series of assumed modes satisfying the geometric boundary conditions of zero slope and curvature at each end:

$$\overline{w}(x,t) = \sum_{k=1}^{N} \overline{a}_k(t) \sin\frac{k\pi x}{a} \tag{2.2}$$

A consistent assumed-mode expression for the in-plane displacement is given by

$$\overline{u}(x,t) = [\overline{b}_R + \overline{b}_0(t)]\frac{x}{a} + \sum_{k=1}^{2N} \overline{b}_k(t) \sin\frac{k\pi x}{a} \tag{2.3}$$

Here $\overline{b}_R$ is the initial panel in-plane displacement at $x = a$ due to the application of the in-plane load $\overline{R}_x$, and $\overline{b}_0(t)$ is the in-plane

displacement at $x = a$ resulting from the subsequent unsteady panel motion. The reasons for dividing the displacement into these two terms will be discussed below.

Following the procedure outlined in Ref. 1, we now wish to derive from Hamilton's principle the Euler-Lagrange equations of motion, the unknowns being the generalized coordinates $\bar{a}_k(t)$, $\bar{b}_R$, $\bar{b}_0(t)$, $\bar{b}_k(t)$ — $3N + 2$ in all. The potential energy of the system is given by

$$W = \frac{1}{2}\int_0^a \left\{ \frac{Eh}{1-\nu^2}\left[\frac{\partial \bar{u}}{\partial x} + \frac{1}{2}\left(\frac{\partial \bar{w}}{\partial x}\right)^2 \right]^2 + D\left(\frac{\partial^2 \bar{w}}{\partial x^2}\right)^2 \right\} dx$$

$$- \left[\bar{R}_x(\bar{b}_R + \bar{b}_0) - \frac{1}{2} K \bar{b}_0^2\right] \tag{2.4}$$

This expression represents physically the strain energy of the panel less the potential of any conservative external loads. In this case the applied in-plane load $\bar{R}_x$ and the load resulting from the spring restraint at $x = a$ both possess potentials. The potential due to $\bar{R}_x$ is positive because a positive $\bar{R}_x$ produces a positive in-plane end displacement, as defined herein; thus $\bar{R}_x$ always does a positive amount of work on the panel. Conversely, the potential due to the restraint spring is negative because the incremental load due to the spring always acts in opposition to the in-plane end displacement. It has been assumed in the formulation above that the spring is not attached until after the load $\bar{R}_x$ is applied; this is a mechanism for allowing in-plane loading to be present in the system even when $K = \infty$. Thus $\bar{b}_R$ represents the end displacement resulting when $\bar{R}_x$ is applied, and $\bar{b}_0$ represents the subsequent in-plane end displacement. It has also been assumed that the panel is initially restrained from buckling if supercritical compressive in-plane loading is applied.

The kinetic energy is given simply by

$$T = \frac{1}{2}\rho_m h \int_0^a \left(\frac{\partial \bar{w}}{\partial t}\right)^2 dx \tag{2.5}$$

Here the kinetic energy associated with both in-plane motion and rotary inertia has been neglected. Since one end of the panel is always firmly fixed, one would expect by far the greater part of the kinetic energy to be associated with transverse motion. In addition, Mindlin (Ref. 2)

has demonstrated that the effects of rotary inertia on flexural motions of a plate are unimportant unless the wavelength of the flexural mode is comparable in magnitude to the thickness of the plate. Wavelengths associated with the critical flutter modes of a panel are generally much larger than the panel thickness, so rotary-inertia effects are safely ignored here.

Finally, the generalized forces are calculated. The generalized force associated with transverse panel displacement is given by

$$(F_z)_k = \int_0^a [-(p - p_\infty) + \overline{\Delta p}] \sin\frac{k\pi x}{a}\, dx, \quad k = 1,2,\ldots,N \tag{2.6}$$

The unsteady pressure difference is obtained from Eq. (2.1). The static pressure difference $\overline{\Delta p}$ is also included; it is positive when the pressure in the undisturbed cavity below the panel exceeds the free-stream static pressure p_∞. The sign convention used for writing the potential of conservative external loads is also applied here. That is, a positive pressure difference $p-p_\infty$ on the exposed surface of the panel opposes motion of the panel in the positive direction, so a minus sign is required where this difference appears. Unsteady cavity effects are not included; in the experiments of interest the panels were mounted so as to eliminate these effects as much as possible. Eqs. (2.6) become then

$$(F_z)_k = -\frac{2q}{M}\int_0^a \left[\frac{1}{U}\frac{\partial \overline{w}}{\partial t} + \frac{\partial \overline{w}}{\partial x} + \frac{(\gamma+1)M}{4}\left(\frac{1}{U}\frac{\partial \overline{w}}{\partial t} + \frac{\partial \overline{w}}{\partial x}\right)^2\right] \sin\frac{k\pi x}{a}\, dx$$

$$+ \int_0^a \overline{\Delta p} \sin\frac{k\pi x}{a}\, dx, \quad k = 1,2,\ldots,N \tag{2.7}$$

The generalized force associated with in-plane panel displacement is then found from the linear portion of Eq. (2.1), multiplied by $\frac{\partial \overline{w}}{\partial x}$ and weighted with the proper assumed mode:

$$(F_x)_k = \frac{2q}{M}\int_0^a \left[\frac{1}{U}\frac{\partial \overline{w}}{\partial t}\frac{\partial \overline{w}}{\partial x} + \left(\frac{\partial \overline{w}}{\partial x}\right)^2\right] \sin\frac{k\pi x}{a}\, dx - \int_0^a \overline{\Delta p}\,\frac{\partial \overline{w}}{\partial x} \sin\frac{k\pi x}{a}\, dx,$$

$$k = 1,2,\ldots,2N \tag{2.8}$$

The assumed-mode series for $\bar{u}$ and $\bar{w}$ are then inserted in the expressions for potential energy, kinetic energy, and generalized forces. The Euler-Lagrange differential equations (see Eqs. (7.39) of Ref. 1) then become, after considerable manipulation,

$$-\frac{\partial W}{\partial \bar{b}_R} = 0 = \bar{R}_x - \frac{Eh}{a(1-\nu^2)}\bar{b}_R \tag{2.9}$$

$$-\frac{\partial W}{\partial \bar{b}_0} = 0 = \bar{R}_x - K\bar{b}_0 - \frac{Eh(\bar{b}_R + \bar{b}_0)}{a(1-\nu^2)} - \frac{\pi^2 Eh}{4a^2(1-\nu^2)}\sum_{n=1}^{N} n^2\bar{a}_n^2 \tag{2.10}$$

(continued next page)

$$-\frac{\partial W}{\partial \bar{b}_k}+(F_x)_k=0=-\frac{Eh}{1-\nu^2}\left[\frac{\pi^2k^2}{2a}\bar{b}_k+\frac{k\pi^3}{8a^2}\left(\sum_{\substack{m,n=1\\ m+n=k}}^{N} mn\bar{a}_m\bar{a}_n+2\sum_{\substack{m,n=1\\ m-n=k}}^{N} mn\bar{a}_m\bar{a}_n\right)\right]+\frac{2q}{M}\left[\frac{\pi}{4U}\left(\sum_{\substack{m,n=1\\ m+n=k}}^{N} m\bar{a}_m\dot{\bar{a}}_n\right.\right.$$

$$\left.\left.-\sum_{\substack{m,n=1\\ m-n=k}}^{N} m\bar{a}_m\dot{\bar{a}}_n+\sum_{\substack{m,n=1\\ n-m=k}}^{N} m\bar{a}_m\dot{\bar{a}}_n\right)+\frac{k\pi}{a}\sum_{m,n=1}^{N}\frac{mn(k^2-m^2-n^2)[1-(-1)^{k+m+n}]}{[k^2-(m-n)^2][k^2-(m+n)^2]}\bar{a}_m\bar{a}_n\right]-\overline{\Delta p}\sum_{n=1}^{N}\frac{kn[1-(-1)^{k+n}]}{k^2-n^2}\bar{a}_n,$$

$$k=1,2,\ldots,2N \tag{2.11}$$

$$-\frac{d}{dt}\left(\frac{\partial T}{\partial \dot{\bar{a}}_k}\right)-\frac{\partial W}{\partial \bar{a}_k}+(F_z)_k=0=-\frac{1}{2}\rho_m ha\ddot{\bar{a}}_k-\frac{Eh}{1-\nu^2}\left[\frac{\pi^2k^2}{2a^2}\bar{b}_0\bar{a}_k+\frac{\pi^3k}{4a^2}\left(\sum_{\substack{m=1\\ m+n=k}}^{N}\sum_{n=1}^{2N} mn\bar{a}_m\bar{b}_n+\sum_{\substack{m=1\\ |m-n|=k}}^{N}\sum_{n=1}^{2N} mn\bar{a}_m\bar{b}_n\right)\right.$$

$$+\frac{\pi^4}{32a^3}\left[4k^2\bar{a}_k\sum_{n=1}^{N}n^2\bar{a}_n^2+4k\sum_{\substack{\ell,m,n=1\\ \ell+m-n=k,\,m\neq n}}^{N}\ell mn\bar{a}_\ell\bar{a}_m\bar{a}_n+2k\left(\sum_{\substack{\ell,m,n=1\\ \ell+m+n=k}}^{N}\ell mn\bar{a}_\ell\bar{a}_m\bar{a}_n+3\sum_{\substack{\ell,m,n=1\\ \ell-m-n=k}}^{N}\ell mn\bar{a}_\ell\bar{a}_m\bar{a}_n\right.\right.$$

$$\left.\left.+\sum_{\substack{\ell,m,n=1\\ m+n-\ell=k}}^{N}\ell mn\bar{a}_\ell\bar{a}_m\bar{a}_n\right)\right]\Bigg]-\frac{D\pi^4k^4}{2a^3}\bar{a}_k-\frac{2q}{M}\sum_{n=1}^{N}\frac{kn[1-(-1)^{k+n}]}{k^2-n^2}\bar{a}_n-\frac{qa}{MU}\dot{\bar{a}}_k+\frac{a[1-(-1)^k]}{k\pi}\overline{\Delta p}$$

$$-\frac{(\gamma+1)q}{2}\left[\frac{k\pi}{a}\sum_{m,n=1}^{N}\frac{mn(k^2-m^2-n^2)[1-(-1)^{k+m+n}]}{[k^2-(m-n)^2][k^2-(m+n)^2]}\bar{a}_m\bar{a}_n+\frac{\pi}{2U}\left(\sum_{\substack{m,n=1\\ m+n=k}}^{N}m\bar{a}_m\dot{\bar{a}}_n-\sum_{\substack{m,n=1\\ m-n=k}}^{N}m\bar{a}_m\dot{\bar{a}}_n+\sum_{\substack{m,n=1\\ n-m=k}}^{N}m\bar{a}_m\dot{\bar{a}}_n\right)\right.$$

$$\left.-\frac{2ka}{\pi U^2}\sum_{m,n=1}^{N}\frac{mn[1-(-1)^{k+m+n}]}{[k^2-(m-n)^2][k^2-(m+n)^2]}\dot{\bar{a}}_m\dot{\bar{a}}_n\right],\quad k=1,2,\ldots,N \tag{2.12}$$

In these equations multiple summations are indicated by a single summation sign, with upper and lower limits of all summation indices given. Exceptions to this convention occur when the upper limits are not equal, in particular in the summations involving products of the $\bar{a}_k$ with the $\bar{b}_k$. When the indices are such that the terms give zero divided by zero, the terms are to be taken as zero.

Eq. (2.9) is seen to give the relationship between the axial elongation or contraction of a plate-column under axial load, with the constraint that no transverse displacement be permitted. Eq. (2.10) is therefore simplified and rearranged to give $\bar{b}_0$ in terms of the transverse-displacement modal amplitudes:

$$\bar{b}_0 = -\frac{\pi^2 Eh}{4a[Eh+Ka(1-\nu^2)]} \sum_{n=1}^{N} n^2 \bar{a}_n^2 \tag{2.13}$$

In similar fashion, Eqs. (2.11) can be rearranged to give the $\bar{b}_k$ in terms of the $\bar{a}_k$. Substituting in Eqs. (2.12) for $\bar{b}_0$ and the $\bar{b}_k$ and rewriting in nondimensional variables produces finally a single set of N quasi-linear, second-order, ordinary differential equations for the N modal amplitudes $a_k(\tau)$:

(see next page)

$$\frac{1}{2}\ddot{a}_k + \frac{1}{2}\pi^2k^2(R_x + \pi^2k^2)a_k + \frac{3}{2}\pi^4k^2\alpha(1-\nu^2)a_k \sum_{n=1}^{N} n^2a_n^2 + \lambda \sum_{n=1}^{N} \frac{kn[1-(-1)^{k+n}]}{k^2-n^2}\, a_n + \frac{1}{2}\left(\frac{\mu\lambda}{M}\right)^{\frac{1}{2}}\dot{a}_k - \frac{[1-(-1)^k]}{k\pi}\,\Delta p$$

$$+ \frac{(\gamma+1)\pi k}{4}\lambda M\frac{h}{a}\sum_{m,n=1}^{N}\frac{mn(k^2-m^2-n^2)[1-(-1)^{k+m+n}]}{[k^2-(m-n)^2][k^2-(m+n)^2]}\,a_m a_n + \frac{(\gamma+1)\pi}{8}\,\frac{h}{a}\,(\mu M\lambda)^{\frac{1}{2}}\Bigg[\sum_{\substack{m,n=1\\ m+n=k}}^{N} m a_m\dot{a}_n + \sum_{\substack{m,n=1\\ m-n=k}}^{N}(na_n\dot{a}_m - ma_m\dot{a}_n)\Bigg]$$

$$- \frac{(\gamma+1)k}{2\pi}\,\mu\,\frac{h}{a}\sum_{m,n=1}^{N}\frac{mn[1-(-1)^{k+m+n}]}{[k^2-(m-n)^2][k^2-(m+n)^2]}\,\dot{a}_m\dot{a}_n + \frac{\pi^2k}{2}\lambda\left(\frac{h}{a}\right)^2\Bigg(\sum_{\substack{\ell,m,n=1\\ k\neq\ell}}^{N}\frac{\ell mn[(k-\ell)^2-m^2-n^2][1-(-1)^{k-\ell+m+n}]}{[(k-\ell)^2-(m-n)^2][(k-\ell)^2-(m+n)^2]}\,a_\ell a_m a_n$$

$$+ \sum_{\ell,m,n=1}^{N}\frac{\ell mn[(k+\ell)^2-m^2-n^2][1-(-1)^{k+\ell+m+n}]}{[(k+\ell)^2-(m-n)^2][(k+\ell)^2-(m+n)^2]}\,a_\ell a_m a_n\Bigg) + \frac{\pi^2k}{8}\left(\frac{\mu\lambda}{M}\right)^{\frac{1}{2}}\left(\frac{h}{a}\right)^2\Bigg[\sum_{\substack{\ell,m,n=1\\ |\ell-(m+n)|=k}}^{N}\frac{\ell m}{m+n}\,a_\ell a_m\dot{a}_n$$

$$+ \sum_{\substack{\ell,m,n=1\\ \ell+m+n=k}}^{N}\frac{\ell m}{m+n}\,a_\ell a_m\dot{a}_n + \sum_{\substack{\ell,m,n=1\\ |\ell-(m-n)|=k,\,m>n}}^{N}\frac{\ell}{m-n}\,a_\ell(na_n\dot{a}_m - ma_m\dot{a}_n) + \sum_{\substack{\ell,m,n=1\\ \ell+m+n=k,\,m>n}}^{N}\frac{\ell}{m-n}\,a_\ell(na_n\dot{a}_m - ma_m\dot{a}_n)\Bigg]$$

$$- \frac{\pi k}{2}\Delta p\left(\frac{h}{a}\right)^2\Bigg(\sum_{\substack{m,n=1\\ k\neq m}}^{N}\frac{mn[1-(-1)^{k-m+n}]}{(k-m)^2-n^2}\,a_m a_n + \sum_{m,n=1}^{N}\frac{mn[1-(-1)^{k+m+n}]}{(k+m)^2-n^2}\,a_m a_n\Bigg) = 0, \quad k = 1,2,\ldots,N \qquad (2.14)$$

With the exception of a slight difference in the definition of α, the terms up to and including the first appearance of Δp are the same as those derived by Dowell (Ref. 3). As was pointed out in Ref. 3, the system parameters for this set of equations are λ, $\frac{\mu}{M}$, $\alpha(1-\nu^2)$, Δp, and R_x. Furthermore, the equations can be recast so as to eliminate the appearance of $\alpha(1-\nu^2)$, so that only one value of $\alpha(1-\nu^2)$ need be considered. With the addition of the nonlinear aerodynamic terms, the situation becomes more complicated. A new parameter, $\frac{h}{a}$, appears explicitly, and μ and M must be specified separately. Also, the explicit dependence on the parameter $\alpha(1-\nu^2)$ can no longer be eliminated. The nonlinear aerodynamic terms appear in the following order: first, those arising from the terms in $(F_z)_k$ dependent on $\left(\frac{\partial \bar{w}}{\partial x}\right)^2$, $\frac{\partial \bar{w}}{\partial x}\frac{\partial \bar{w}}{\partial t}$, and $\left(\frac{\partial \bar{w}}{\partial t}\right)^2$, respectively; secondly, those arising from the terms in $(F_x)_k$ dependent on $\left(\frac{\partial \bar{w}}{\partial x}\right)^2$, $\frac{\partial \bar{w}}{\partial x}\frac{\partial \bar{w}}{\partial t}$, and $\overline{\Delta p}\,\frac{\partial \bar{w}}{\partial x}$, respectively. Note also that the terms due to the nonlinear part of $(F_z)_k$ depend linearly on $\frac{h}{a}$ and are quadratic in the a_k, while those due to $(F_x)_k$ depend quadratically on $\frac{h}{a}$ and are cubic in the a_k.

Eqs. (2.14) are integrated numerically with respect to the dimensionless time τ from given initial conditions. The calculations are performed on an IBM 360/67 computer. A subroutine based on the Kutta-Merson procedure is used, and the step size is varied in order to keep the relative error within given bounds. Provision is also made for including or excluding in the computation any of the nonlinear aerodynamic terms, as desired.

2.2 Comparison with Previous Results

In order to check the numerical integration, a few test cases were run with linear aerodynamic loading, and the results were compared with those from Ref. 3. Figs. 2 and 3 show the dimensionless panel displacement at the three-quarter chord vs. dimensionless time for values of system parameters noted on the figures. Fig. 2 corresponds directly to Fig. 2 of Ref. 3, and the limit-cycle amplitude taken from Fig. 3 checks that given in Fig. 5 of Ref. 3. All the other test cases showed similar good agreement.

2.3 Behavior with Zero System Damping

Some interesting and unanticipated problems were encountered when the equations with linear aerodynamic loading were solved for zero system damping. Figs. 4 and 5 show the panel response for the same set of initial conditions and system parameters used for Figs. 2 and 3, except that $\mu = 0$. After an initial transient shown in Fig. 4, the response becomes periodic but not simple harmonic, as is evidenced in Fig. 5. The response curve illustrated in Fig. 5 continues indefinitely without change, and the peak amplitude is different from that shown in Fig. 3. That the system does demonstrate instability for this set of parameters is illustrated in Fig. 6. Here the initial displacement at the three-quarter chord is smaller than that in Figs. 2-5 by a factor of approximately four, and the amplitude clearly grows with time. It then decreases, and the same process is repeated again (but is not shown here). Note also that the maximum amplitudes are different for the different initial conditions. This does not mean, however, that a unique limit-cycle amplitude and frequency are not associated with a given set of (supercritical) system parameters. In Fig. 7, the panel response is shown for $N = 2$ and for supercritical system parameters. The initial conditions in this case were obtained from a harmonic-balance solution. It is seen that there is no initial transient, and the panel response continues at the same amplitude. Solutions for other values of system parameters exhibit the same behavior, and it can therefore be concluded that the method of calculating the panel motion with time will produce a limit cycle of constant amplitude for zero system damping only if the initial conditions correspond exactly to the limit-cycle modal amplitudes. For any other initial conditions, the panel oscillates between stable and unstable states. If, on the other hand, the system parameters are subcritical, the panel will oscillate without decaying, and the peak amplitude is determined by the initial conditions. Figs. 8 and 9 show the panel displacement at the three-quarter chord for a subcritical value of λ and different initial conditions. Here it will be observed that the peak amplitudes never exceed the initial amplitudes, although the motion is not simple harmonic.

These results can also be interpreted with the aid of some general stability considerations for autonomous systems (Ref. 4). The panel equations for zero system damping describe a system whose state is uniquely determined by the $2N$ modal amplitudes and velocities a_k, $\dot{a}_k$, $k = 1,2,\cdots,N$, or in other words by a point in the $2N$-dimensional space E_a^{2n}. The origin of this space is clearly an equilibrium point — it corresponds to the panel in a flat, undisturbed state — and it is desired to examine the stability of the panel in the neighborhood of this state. In brief, the origin is stable if for <u>any</u> sphere $S(R)$ of radius R in E_a^{2n}, centered on the origin, there exists another sphere $S(r)$ of radius $r \leqq R$ such that any motion originating in $S(r)$ remains in $S(R)$ ever after. This stable behavior is exhibited in Figs. 8 and 9. Reducing the initial amplitude reduces the maximum resultant amplitude, so for any given bound on the amplitude the initial amplitude can be reduced to keep the resultant motion within the bound. On the other hand, if such a sphere $S(r)$ cannot be found, the origin is unstable. Figs. 4, 5, and 6 illustrate this unstable situation. It is evident that there is an amplitude that the resultant motion will exceed, no matter how small (but finite) the initial amplitude is. These same conclusions can be drawn when the initial conditions are broadened to include nonzero initial velocities, and the reader is referred to Ref. 4 for the full, precise definitions of stability and instability.

2.4 Effects of Aerodynamic Nonlinearities

As has been pointed out many times in the past, the geometric panel nonlinearity is a stabilizing factor, in that the increase of in-plane tension with tranverse displacement serves to limit the supercritical response amplitudes. On the other hand, aerodynamic nonlinearities are in general destabilizing, in the sense that they act to increase supercritical response amplitudes and in extreme cases can even lead to panel instabilities for values of system parameters that would be subcritical on the basis of a theory with linear aerodynamic relations. Refs. 5 and 6 are typical examples of other studies of the effects of aerodynamic nonlinearities. Ref. 5 presents results for a panel (plate-column) on hinged supports with variable in-plane restraint. Third-order piston theory is used for the aerodynamic loads, and the flow is taken over both sides of the panel, so that the only aerodynamic nonlinear term is the cubic one. It was demonstrated with a two-mode harmonic-balance solution that for certain values of in-plane restraint (intermediate between no restraint at all and infinte restraint) an instability could occur below the linear stability boundary if the initial amplitude were large enough. However, the parameter values used in these calculations give for an aluminum panel at sea level a thickness-to-chord ratio $\frac{h}{a}$ of 0.0131 and a Mach number of 28.4. These values, coupled with the assumption of two-sided flow, give a rather unrealistic situation. On the other hand, Ref. 6 gives results for much more reasonable physical constants — a steel plate at sea level, with a length-to-width ratio of three, a thickness-to-chord ratio of $\frac{1}{400}$, and critical Mach numbers from two to four. One-sided flow is assumed, and second-order piston theory is used for the aerodynamic loads. The calculations, though, show that the region of stability is increased as the initial disturbance increases, so that the critical speed goes from 952 meters per second for the linear theory to 1600 meters per second for $a_1(0) = -a_2(0) = 1.0$. The transverse displacement is approximated with two chordwise modes and one spanwise mode, and the supports are hinged. Solutions are found by direct integration over time of the equations for the modal amplitudes. In both Ref. 5 and Ref. 6 the panel geometric nonlinearity is taken into account with the Kármán approximation.

In this investigation the effects of aerodynamic nonlinearities were first introduced by considering only the term from $(F_z)_k$ proportional to $\left(\frac{\partial \bar{w}}{\partial x}\right)^2$. A single new system parameter, $\frac{Mh}{a}$, is required. Figs. 10 and 11 illustrate the effect of this term. The value of λ chosen is subcritical from the viewpoint of linear theory, and α is set equal to zero, so that the stabilizing effect of the panel geometric nonlinearity is not present. In Fig. 10, the panel is observed to be stable for $a_1(0) = -a_2(0) = 1.71$, while in Fig. 11 a divergent instability occurs for $a_1(0) = -a_2(0) = 1.72$. Aside from stability considerations, another important effect observed with this quadratic nonlinearity is its impact on transient panel motion. Figs. 12 and 13 illustrate the marked difference in panel response caused by the introduction of this nonlinear term; in both cases the panel is stable, but with the aerodynamic nonlinearity in the equations the response peaks are higher, and the shape of the curve in spots differs greatly from that obtained with linear aerodynamic terms.

III. PANEL ON CLAMPED SUPPORTS

In Ref. 7 are described some high-Mach-number panel-flutter experiments, where in-plane tension was used to stabilize a clamped panel in a wind tunnel until stable flow conditions were established. Then the tension was reduced until the panel fluttered. As soon as the onset of flutter was perceived, the tension was increased again until the flutter stopped. The tension at which the flutter stopped was greater than the tension required to stabilize the panel initially. In an attempt to duplicate this "hysteresis" phenomenon theoretically, the equations of motion for a clamped panel, with both aerodynamic and geometric nonlinearities, have been derived in a manner similar to that described in Section II. The in-plane applied load $\bar{R}_x$ is an arbitrary function of time. Temperature effects are also taken into account by including a temperature-difference term with both temporal and spatial variation, and a distributed mass is placed at one end to account for any inertial effects from the tensioning mechanism.

Inasmuch as numerical results are not yet available, a detailed discussion of this problem will be deferred until there are some specific data on which to comment.

IV. METHODS OF SOLUTION

In accordance with the research proposal, a specific pilot problem has been investigated that demonstrates an inherent weakness of the Galerkin procedure when it is applied to the solution of differential equations in a purely mathematical sense. Consider the clamped Timoshenko beam (Ref. 8) illustrated in Fig. 14. The equation for harmonic lateral vibrations, without rotary-inertia effects, can be written as

$$EI\frac{d^4\tilde{w}}{dx^4} + \frac{EI}{D_Q}\rho_m\omega^2\frac{d^2\tilde{w}}{dx^2} - \rho_m\omega^2\tilde{w} = 0 \tag{4.1}$$

The lateral deflection has been written as

$$\bar{w}(x,t) = \tilde{w}(x)e^{i\omega t} \tag{4.2}$$

Let

$$\tilde{w}(x) = A(1-\cos\frac{2\pi x}{a}) \tag{4.3}$$

so that all boundary conditions (in this case all geometric in nature) are satisfied. The Galerkin integral for determining the existence of the amplitude parameter A is found by substituting Eq. (4.3) into Eq. (4.1), weighting the resultant equation with the assumed mode in Eq. (4.3), and integrating over the length of the beam:

$$A\int_0^a\Big[-EI\Big(\frac{2\pi}{a}\Big)^4\cos\frac{2\pi x}{a} + \frac{EI}{D_Q}\rho_m\omega^2\Big(\frac{2\pi}{a}\Big)^2\cos\frac{2\pi x}{a} - \rho_m\omega^2(1-\cos\frac{2\pi x}{a})\Big](1-\cos\frac{2\pi x}{a})\,dx = 0 \tag{4.4}$$

If A exists, the eigenvalue is

$$\omega^2 = \frac{16\pi^4 EI/3\rho_m a^4}{1 + 4\pi^2 EI/3D_Q a^2} \tag{4.5}$$

Now, if the same problem is approached via the potential-energy method, the total potential of the system includes the energy of bending, the energy of shearing, and the kinetic energy of vibration. Thus,

$$W - T = \frac{EI}{2}\int_0^a \left(\frac{d^2\tilde{w}}{dx^2} - \frac{1}{D_Q}\frac{d\tilde{Q}}{dx}\right)^2 dx + \frac{1}{2}\int_0^a \frac{\tilde{Q}^2}{D_Q}\,dx - \frac{1}{2}\rho_m\omega^2\int_0^a \tilde{w}^2\,dx \tag{4.6}$$

The direct method of the calculus of variations (the Rayleigh-Ritz method) requires that assumed modes satisfying the geometric boundary conditions be selected when the functional to be minimized is the total potential energy, so the assumed modes are taken as

$$\tilde{w}(x) = A\left(1-\cos\frac{2\pi x}{a}\right) \tag{4.7}$$

$$\tilde{Q}(x) = B\sin\frac{2\pi x}{a} \tag{4.8}$$

The shear-force amplitude $\tilde{Q}$ is used here instead of the shear-angle amplitude, since the shear-angle amplitude is simply $\frac{\tilde{Q}}{D_Q}$, and a direct proportion exists.

Enforcement of the condition $\delta(W-T) = 0$ with respect to both A and B yields two simultaneous equations for ensuring the existence of A and B. The resulting characteristic equation gives the eigenvalue

$$\omega^2 = \frac{16\pi^4 EI/3\rho_m a^4}{1 + 4\pi^2 EI/D_Q a^2} \tag{4.9}$$

Note that this result, which represents a minimum-energy solution, is different from the Galerkin solution, Eq. (4.5), which represents only an approximate solution to a differential equation. The reason for this discrepancy is that the Timoshenko-beam equation, Eq. (4.1), is not an Euler equation. Actually, variation of Eq. (4.6) with respect to both $\tilde{w}$ and $\tilde{Q}$ produces two Euler equations. Eliminating $\tilde{Q}$ in these equations leads to a single governing equation in $\tilde{w}$, Eq. (4.1). Interestingly enough, in the case of simple supports, no difference exists between the two methods of solution; however, for clamped supports, a Galerkin solution producing the same results as the minimum-energy solution can only be obtained if the two Euler equations governing the problem are utilized. In the present problem, the discrepancy is serious, since the Galerkin solution underestimates the effect of transverse shear. This problem is more serious in the case of

sandwich beams, where the transverse shear is extremely important. It is also interesting to note that a similar problem, with similar conclusions, was considered independently by Yu and Lai (Ref. 9).

The foregoing pilot problem indicates that continuing results on more complicated problems may lead to reevaluation of the methods and results associated with nonconservative nonlinear problems on panels having curvature and boundary restraints other than simple supports.

V. CONCLUDING REMARKS

Further research activity will be concentrated in the following areas:

(1) Work begun with the panel on hinged supports will be continued in an effort to assess systematically the effects of aerodynamic nonlinearities on panel response and stability.

(2) Numerical results for the clamped panel will be obtained for a varying in-plane load and temperature difference corresponding as closely as possible to the environment of the panels used in the experiments of Ref. 7. Additional studies on the order of those discussed above for the panel on hinged supports will also be performed.

(3) The methods developed for analyzing the infinite-span panel will be extended to take into account finite-span effects, and the influence of such additional system parameters as aspect ratio, spanwise curvature, and finite-edge boundary conditions will be determined.

(4) Experience with the results from the method of analysis described herein has shown that they are very useful for studying in detail the panel motion for a particular case but often inefficient in providing information for, say, a parameter survey. New and potentially valuable approaches based on examining the energy of the system (Ref. 10, for example) show promise in alleviating this problem. Further effort will therefore be devoted to examining in detail the energy interchange between panel and airstream as a means of testing these new ideas.

(5) One important aerodynamic nonlinear effect, that of the unsteady boundary layer at the panel surface, has heretofore been neglected in this research program. Approximate means of taking into account the effects of a boundary layer on an oscillating surface have been developed for infinite-span panels of both infinite and finite chord (Ref. 11, for example). This work will be reviewed, and improved methods of analysis for the two-dimensional and the three-dimensional problem will be sought.

REFERENCES

1. McIntosh, S.C., Jr., "Preliminary Theoretical Considerations of Some Nonlinear Aspects of Hypersonic Panel Flutter," Annual Report, NASA Grant NGR 05-020-102, 31 August 1965 to 1 September 1966, Dept. of Aeronautics and Astronautics, Stanford University, Stanford, Calif.

2. Mindlin, R.D., "Influence of Rotatory Inertia and Shear on Flexural Motions of Isotropic, Elastic Plates," Journal of Applied Mechanics, Vol. 18, No. 1, March 1951, pp. 31-38.

3. Dowell, E.H., "Nonlinear Oscillations of a Fluttering Plate," AIAA Journal, Vol. 4, No. 7, July 1966, pp. 1267-1275.

4. La Salle, J. and Lefschetz, S., Stability by Liapunov's Direct Method With Applications, Academic Press, New York, 1961, pp. 30-33.

5. Bolotin, V.V., Gavrilov, Iu.V., Makarov, B.P., and Shveiko, Iu.Iu., "Nonlinear Problems of the Stability of Plane Panels at Hypersonic Speeds," Izv. Akad. Nauk SSSR, OTN, Mekh. i Mashino., No. 3, 1959, pp. 59-64.

6. Stepanov, R.D., "Problems of Plate Flutter in Nonlinear Arrangement," FTD-TT-64-596, April 1965, Foreign Technology Division, Air Force Systems Command, Wright-Patterson Air Force Base, Ohio; translated from Izv. Vyssh. Ucheb. Zav., Mashino., No. 12, 1960, pp. 46-54.

7. Ketter, D.J. and Voss, H.M., "Panel Flutter Analyses and Experiments in the Mach Number Range of 5.0 to 10.0," FDL-TDR-64-6, March 1964, Air Force Flight Dynamics Laboratory, Research and Technology Division, Air Force Systems Command, Wright-Patterson Air Force Base, Ohio.

8. Timoshenko, S., Vibration Problems in Engineering, Van Nostrand, New York, 1928.

9. Yu, Y.-Y. and Lai, J.-L., "Application of Galerkin's Method to the Dynamic Analysis of Structures," AIAA Journal, Vol. 5, No. 4, April 1967, pp. 792-794.

10. Roorda, J. and Nemat-Nasser, S., "An Energy Method for Stability Analysis of Nonlinear, Nonconservative Systems," AIAA Journal, Vol. 5, No. 7, July 1967, pp. 1262-1268.

11. Zeydel, E.F.E., "Study of the Pressure Distribution on Oscillating Panels in Low Supersonic Flow with Turbulent Boundary Layer," CR-691, February 1967, NASA, Washington, D.C.

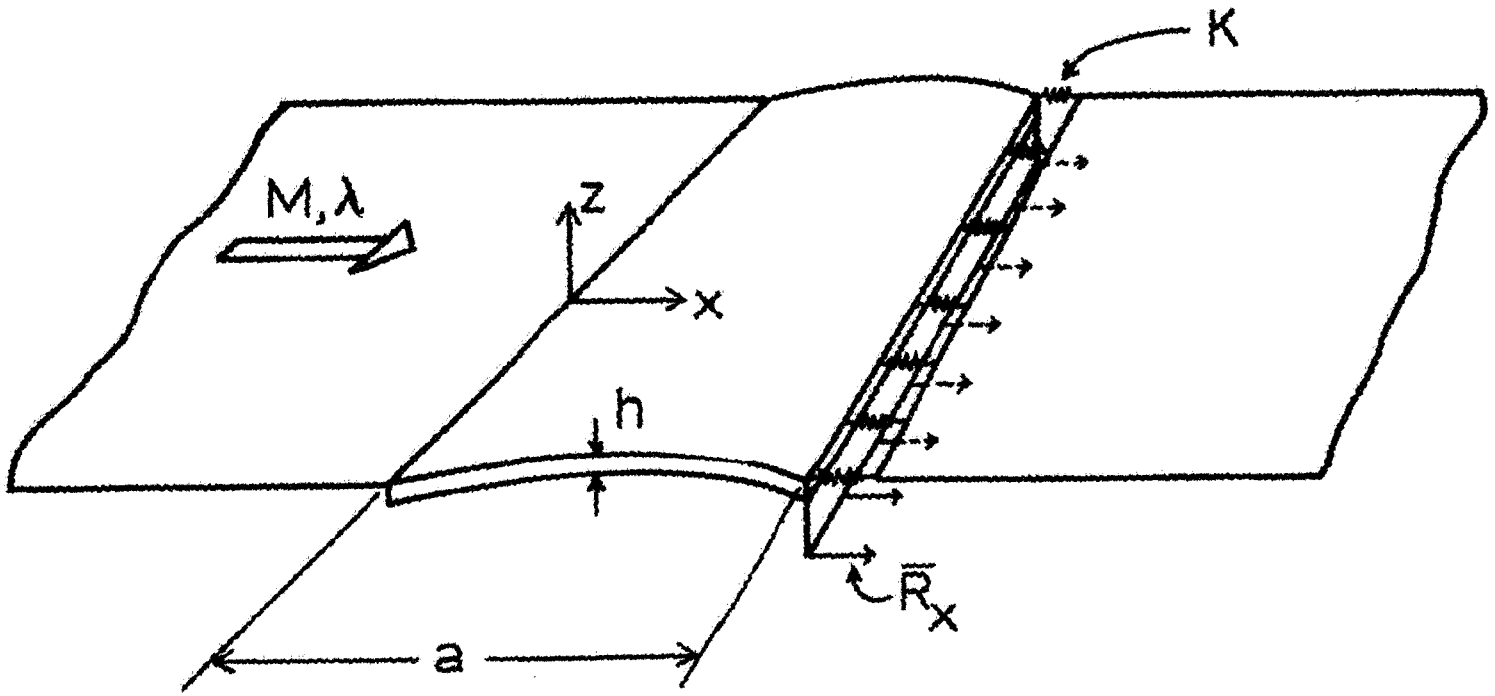

Figure 1. Two-dimensional panel (plate-column) on hinged supports.

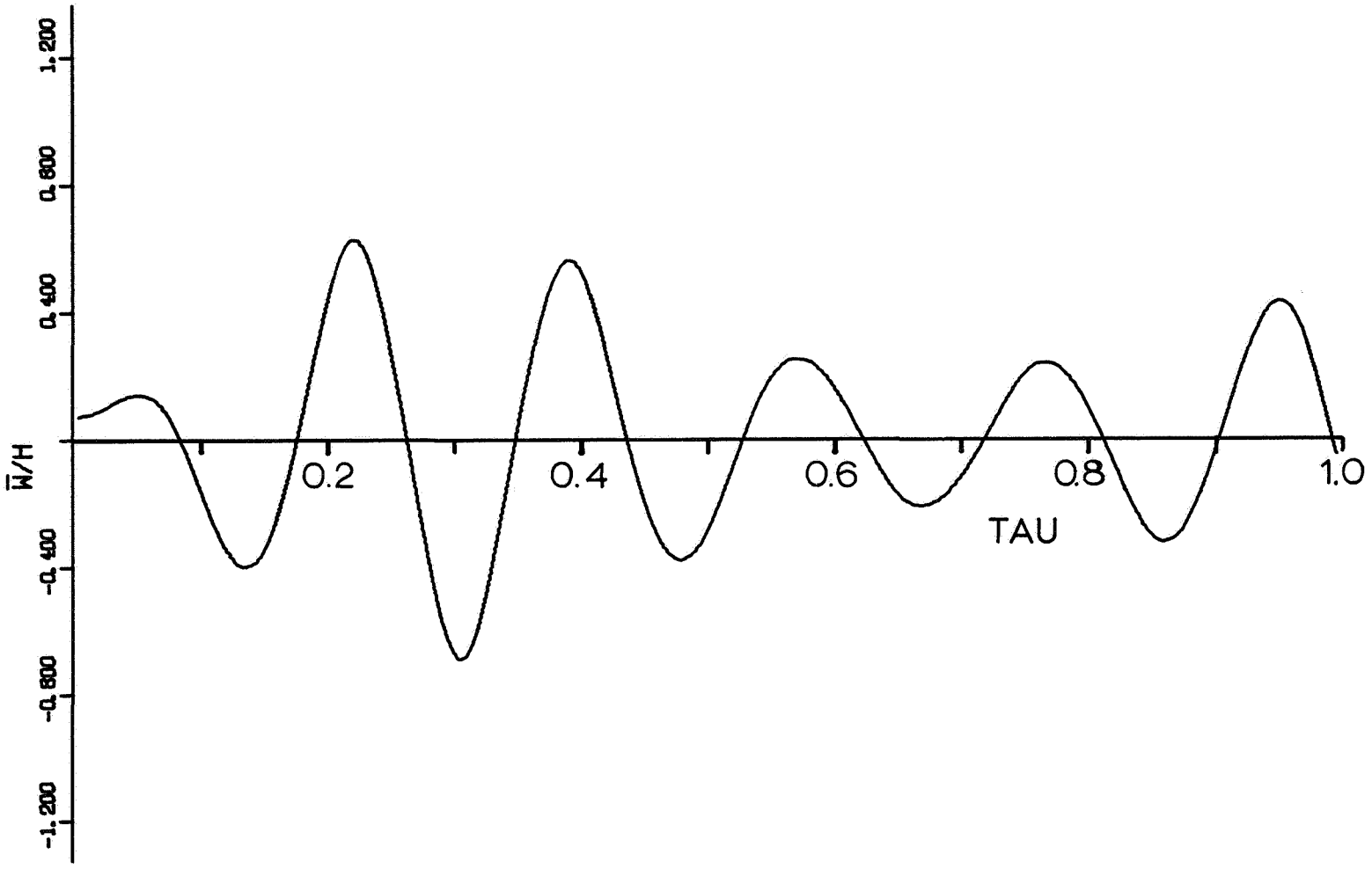

Figure 2. Dimensionless panel displacement at $x = 0.75a$ vs. dimensionless time τ; $\lambda = 400$, $\frac{\mu}{M} = 0.01$, $\alpha = 1.0$, $N = 6$, $a_1(0) = 0.1$, linear aerodynamic terms.

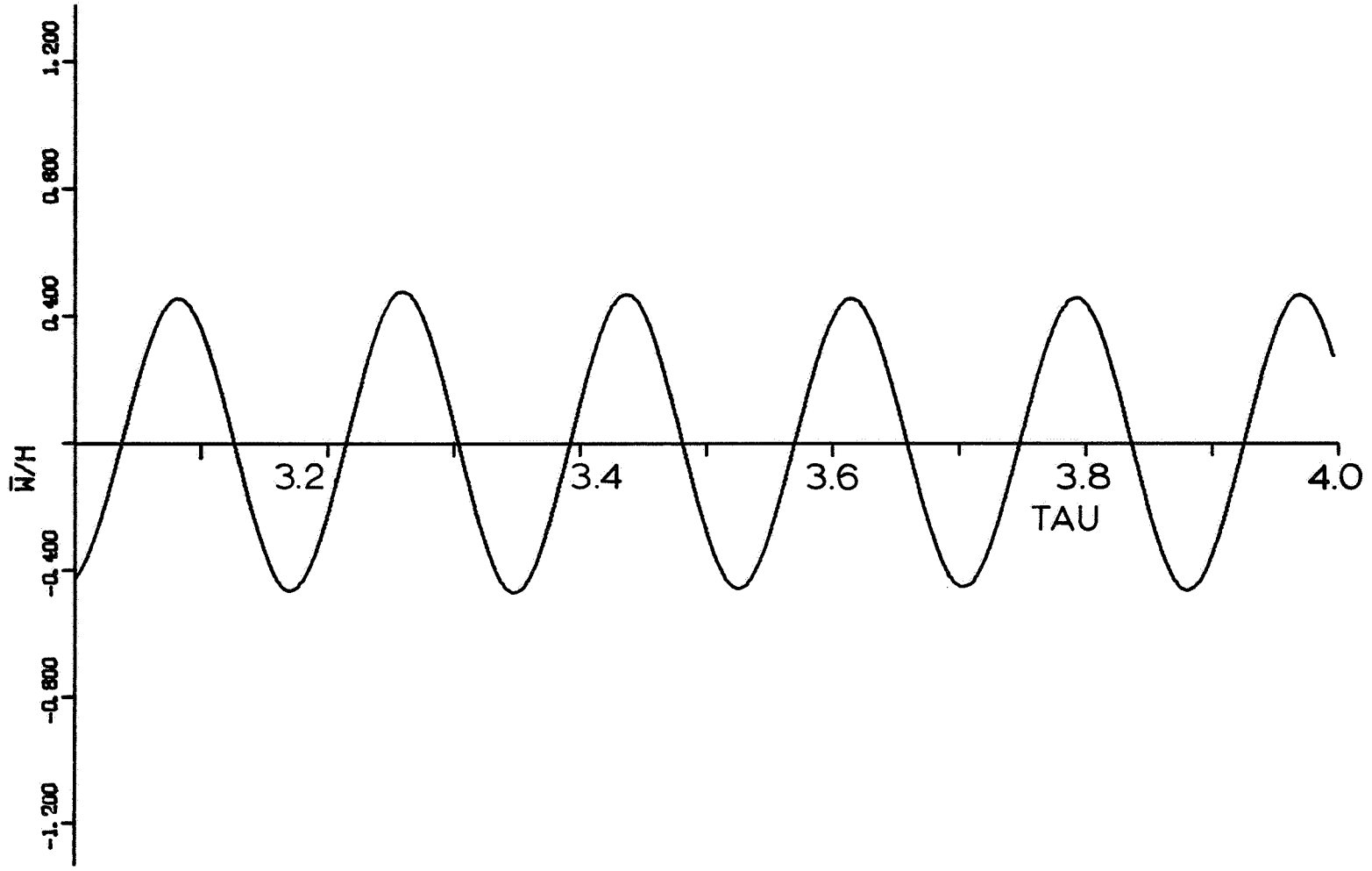

Figure 3. Continuation, response of panel of Fig. 2.

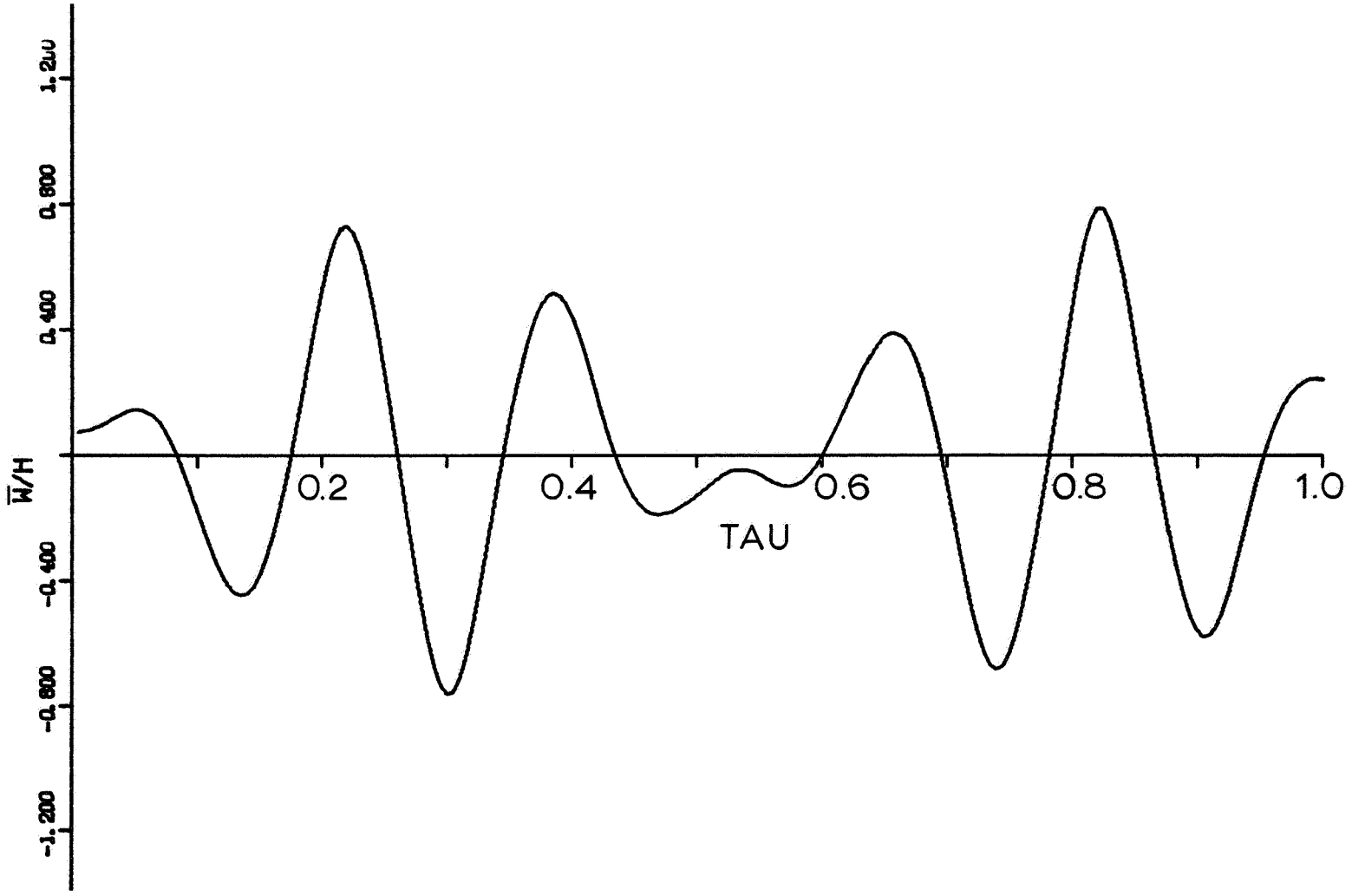

Figure 4. Dimensionless panel displacement at $x = 0.75a$ vs. dimensionless time τ for zero system damping; $\lambda = 400$, $\frac{\mu}{M} = 0.0$, $\alpha = 1.0$, $N = 6$, $a_1(0) = 0.1$, linear aerodynamic terms.

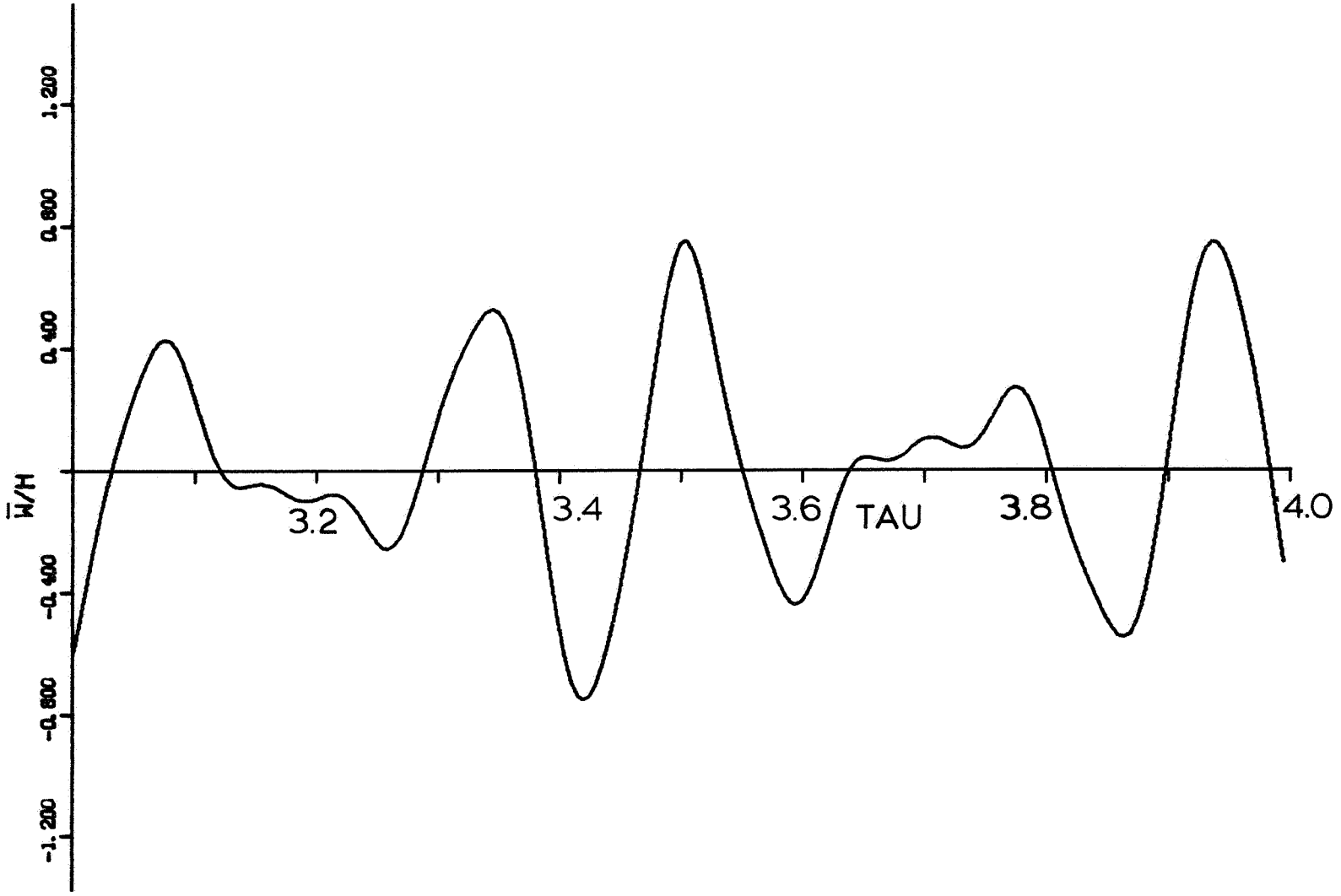

Figure 5. Continuation, response of panel of Fig. 4.

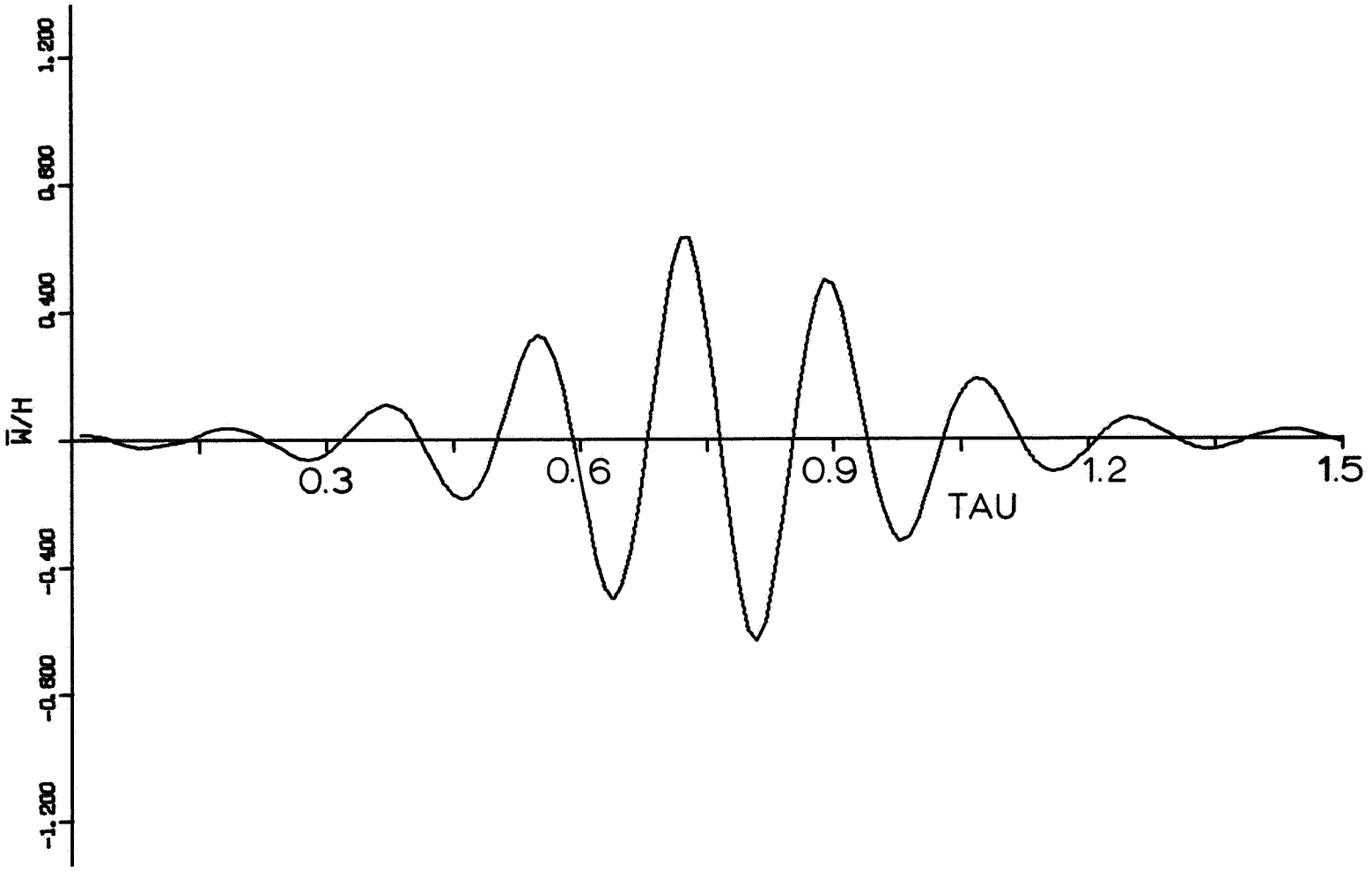

Figure 6. Dimensionless panel displacement at $x = 0.75a$ vs. dimensionless time τ for zero system damping; $\lambda = 400$, $\frac{\mu}{M} = 0.0$, $\alpha = 1.0$, $N = 6$, $a_1(0) = -a_2(0) = 0.01$, linear aerodynamic terms.

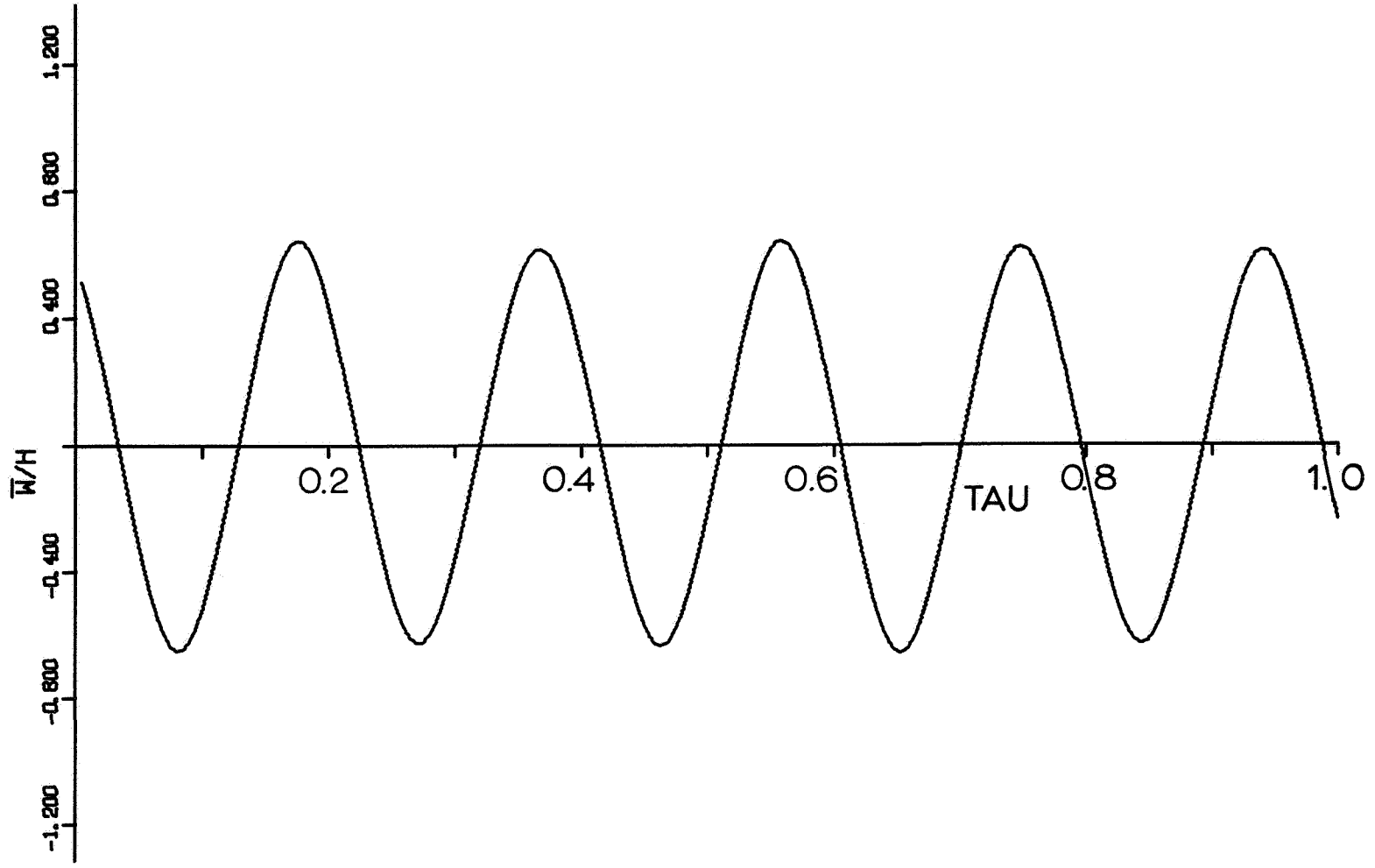

Figure 7. Dimensionless panel displacement at $x = 0.75a$ vs. dimensionless time τ for zero system damping; $\lambda = 346.1$, $\frac{\mu}{M} = 0.0$, $\alpha = 1.0$, $N = 2$, $a_1(0) = -a_2(0) = 0.363$, linear aerodynamic terms.

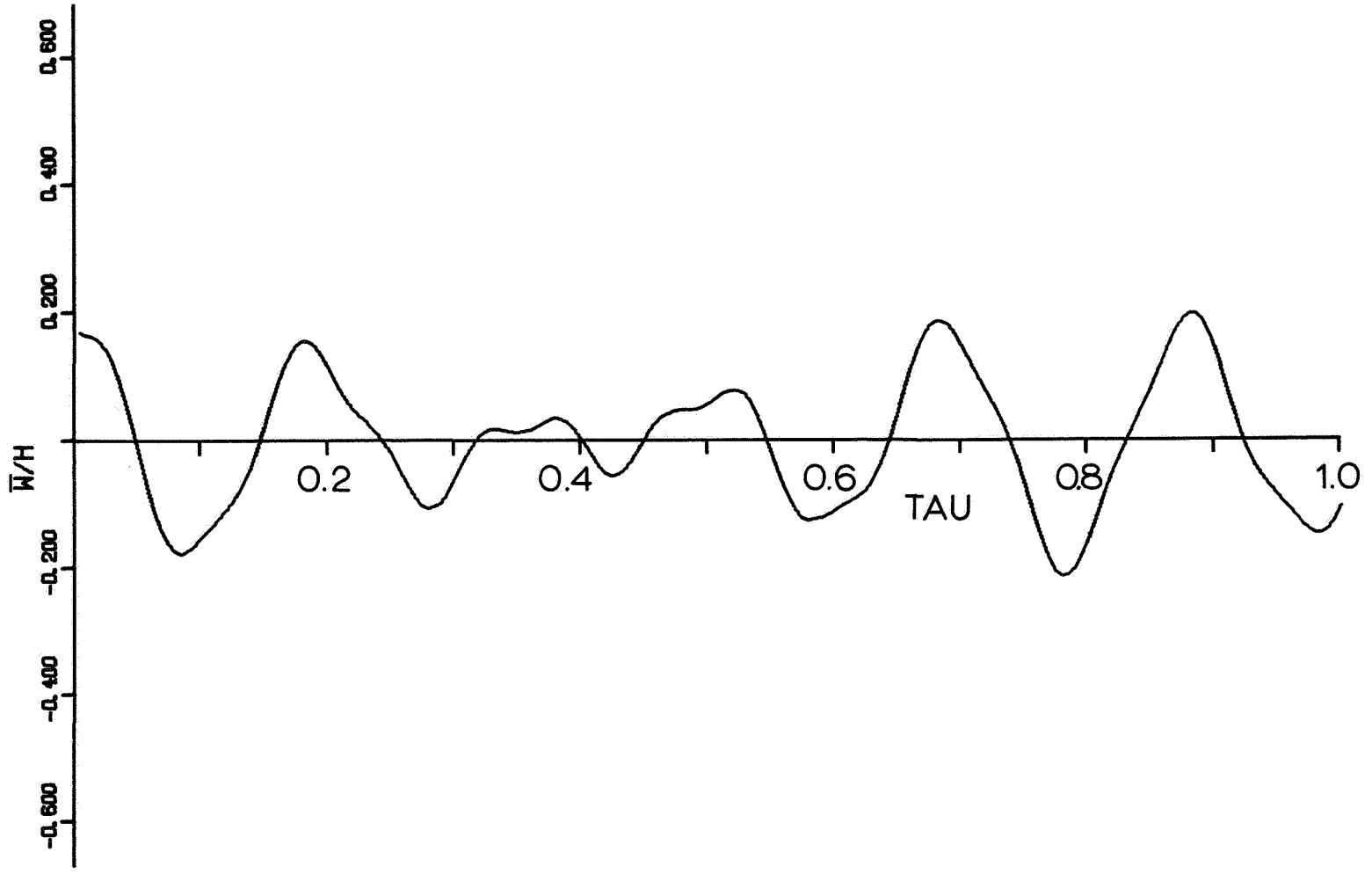

Figure 8. Dimensionless panel displacement at $x = 0.75a$ vs. dimensionless time τ for zero system damping and subcritical λ; $\lambda = 330$, $\frac{\mu}{M} = 0.0$, $\alpha = 1.0$, $N = 6$, $a_1(0) = -a_2(0) = 0.1$, linear aerodynamic terms.

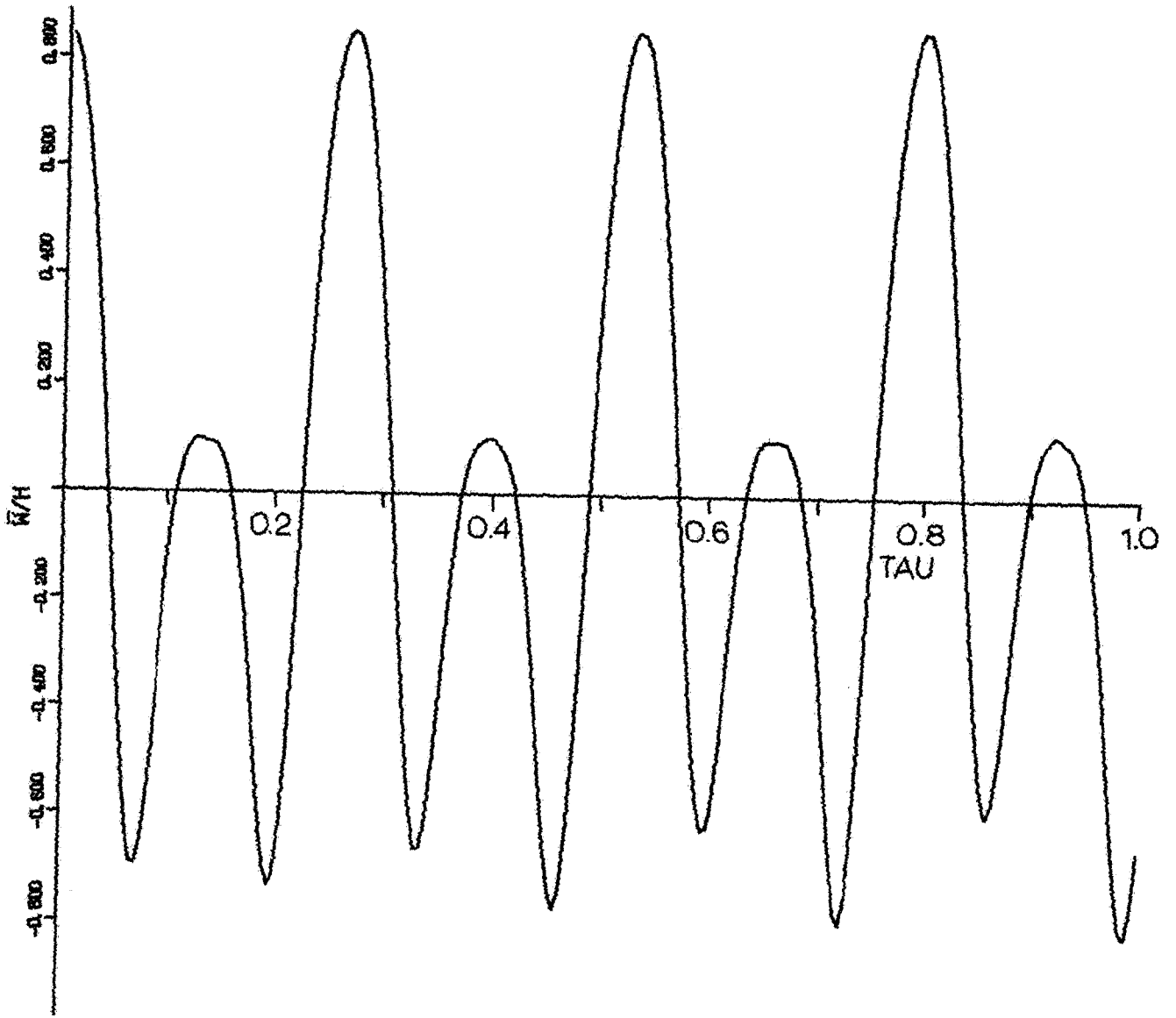

Figure 9. Response of panel of Fig. 8 with different initial conditions — $a_1(0) = -a_2(0) = 0.5$.

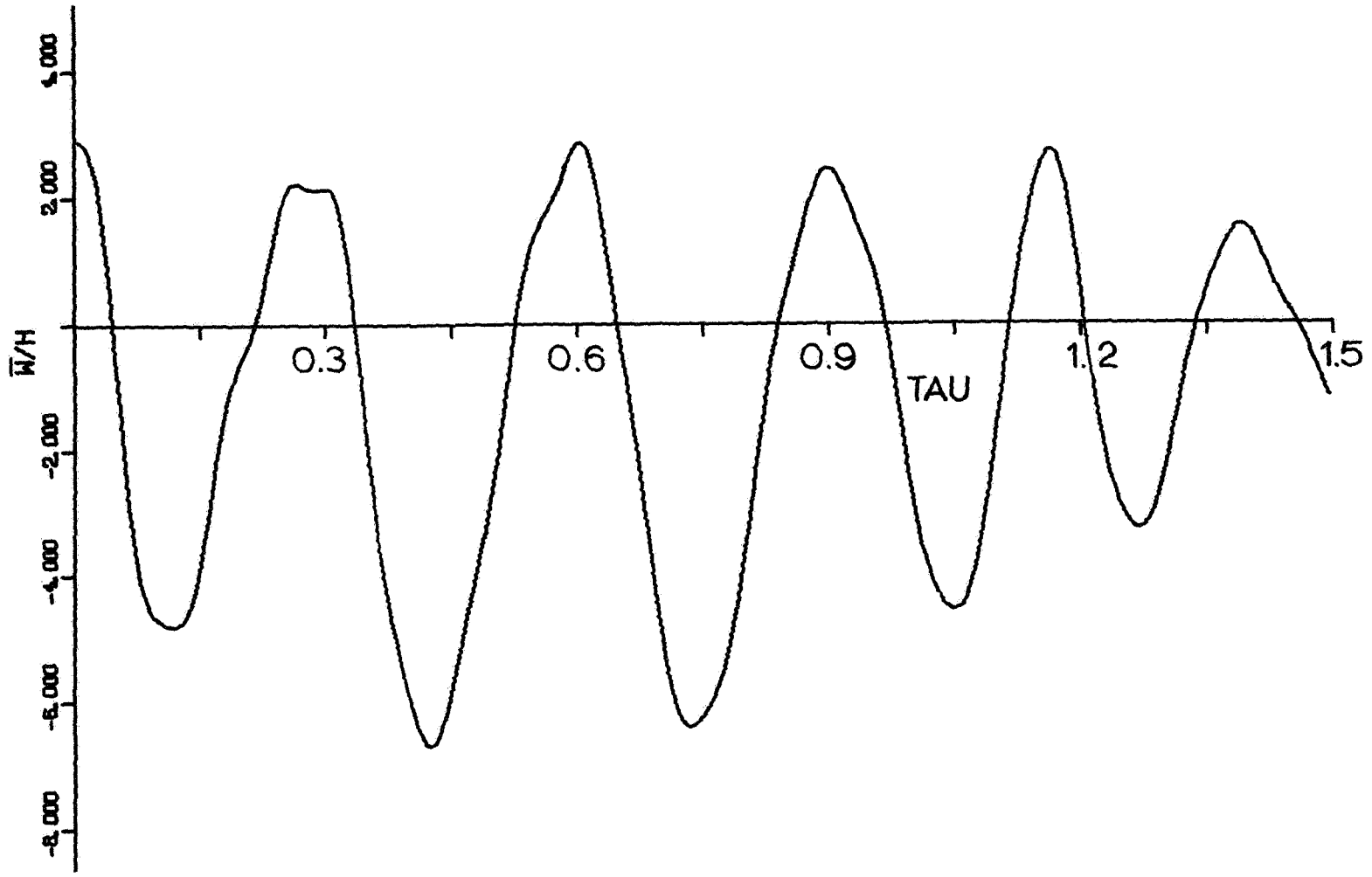

Figure 10. Dimensionless panel displacement at $x = 0.75a$ vs. dimensionless time τ; $\lambda = 330$, $\frac{\mu}{M} = 0.01$, $\alpha = 0.0$, $N = 6$, $\frac{Mh}{a} = 0.05$, $a_1(0) = -a_2(0) = 1.71$, linear aerodynamic terms plus term proportional to $\left(\frac{\partial \bar{w}}{\partial x}\right)^2$ from $(F_z)_k$.

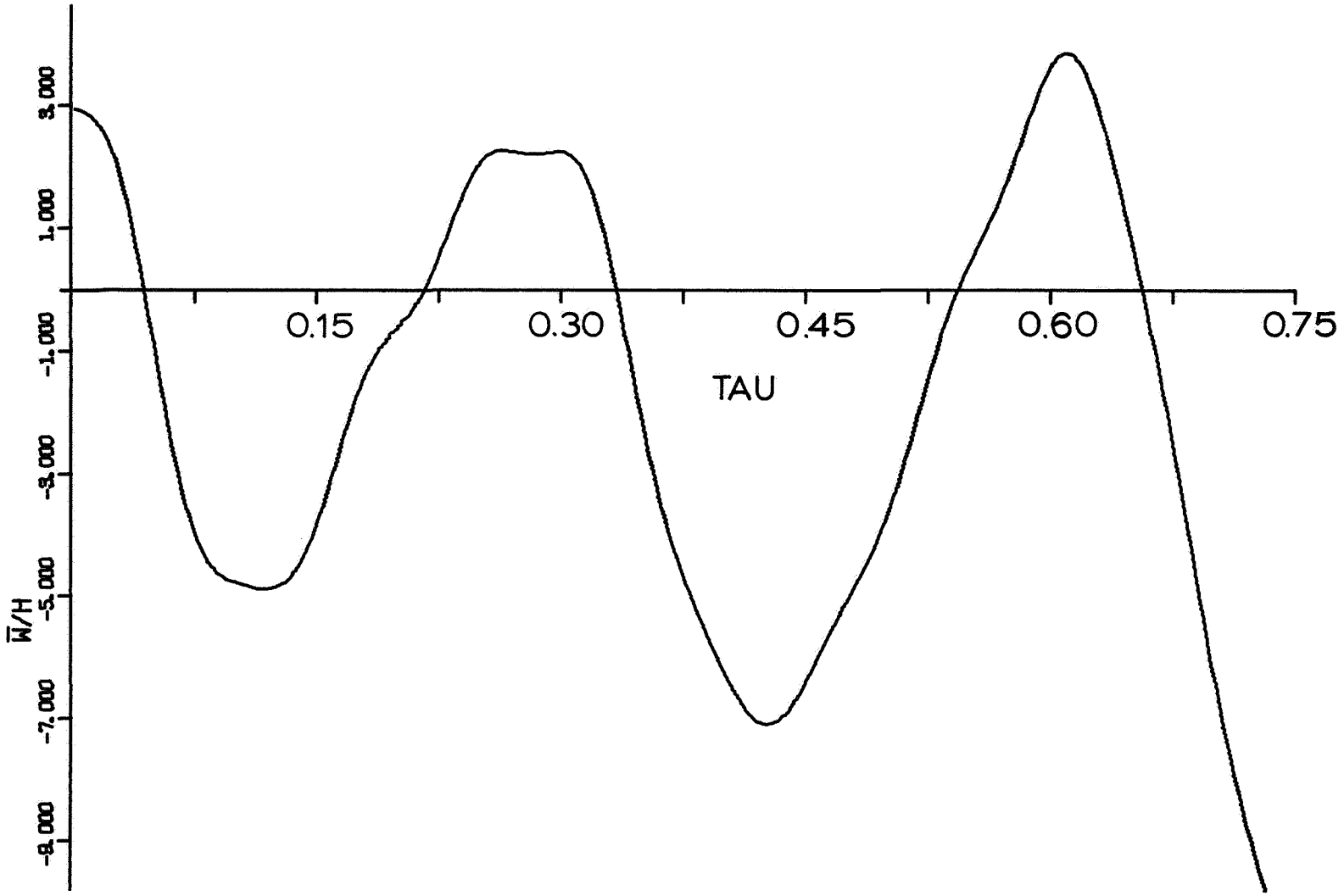

Figure 11. Response of panel of Fig. 10 with slightly greater initial conditions — $a_1(0) = -a_2(0) = 1.72$.

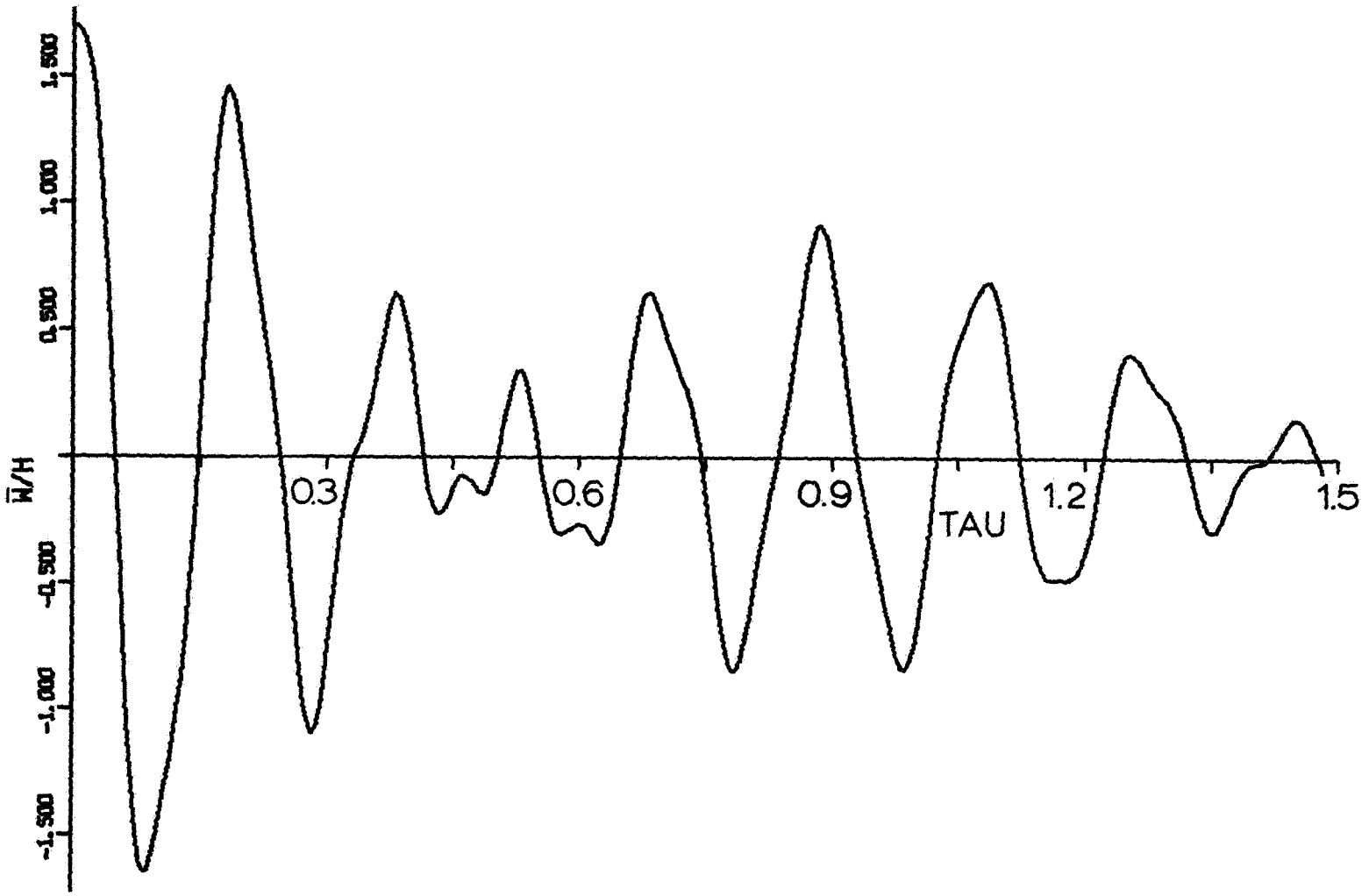

Figure 12. Response of panel of Fig. 10 with diminished initial conditions and linear aerodynamic terms — $\lambda = 330$, $\frac{\mu}{M} = 0.01$, $\alpha = 0.0$, $N = 6$, $a_1(0) = - a_2(0) = 1.0$.

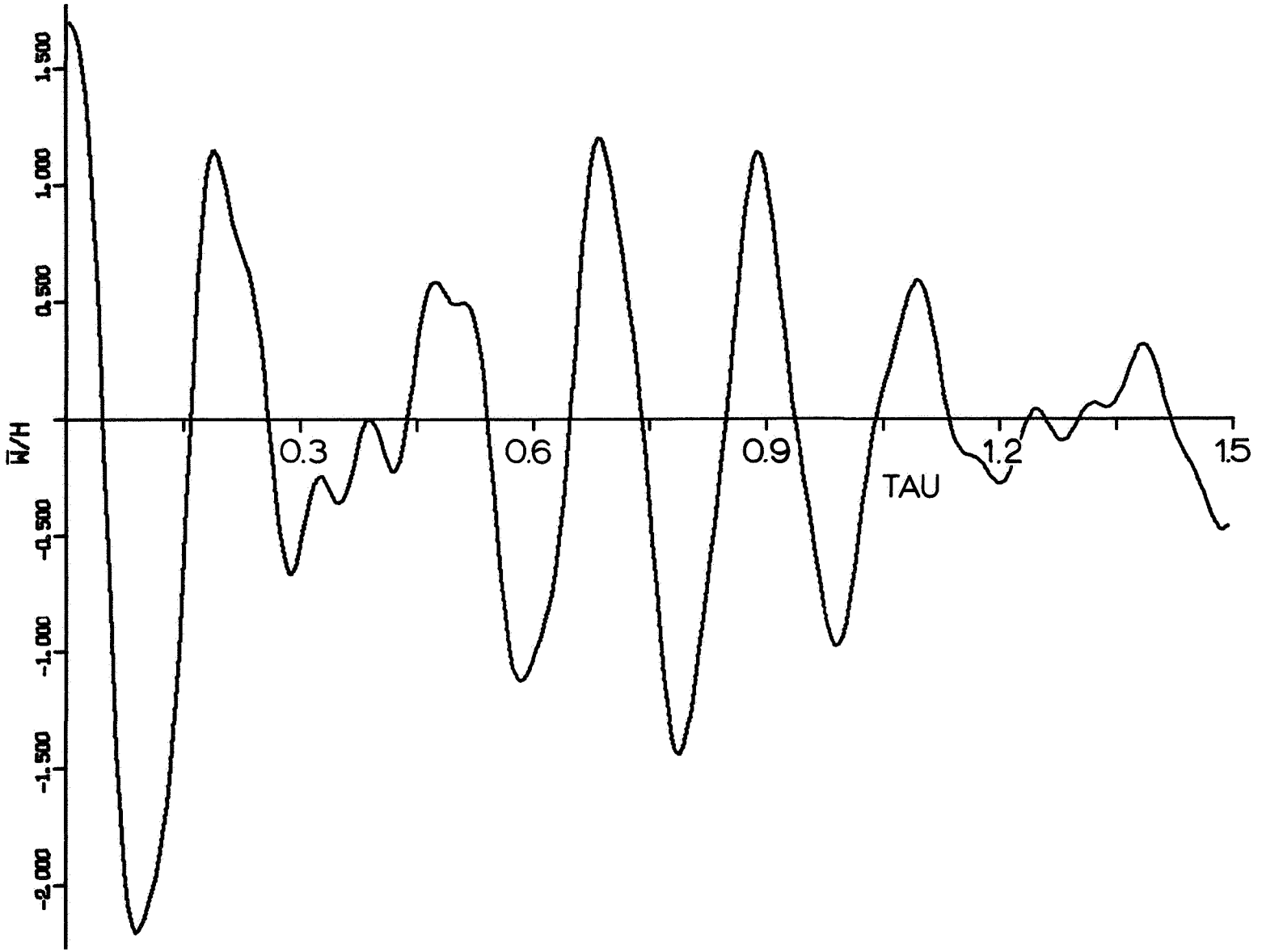

Figure 13. Response of panel of Fig. 12, with same initial conditions and linear aerodynamic terms plus term proportional to $\left(\frac{\partial \bar{w}}{\partial x}\right)^2$ from $(F_z)_k$.

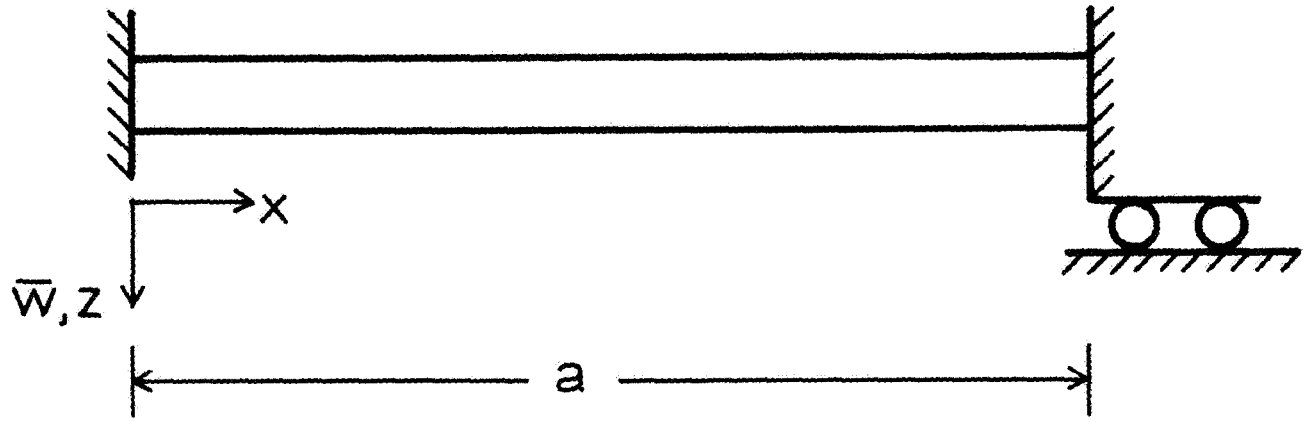

Figure 14. Timoshenko beam on simple supports.